as primary reaction products. $VOC_2H_4^+$ then reacts rapidly to form $VOC_4H_6^+$ and $VOC_4H_8^+$. The $VOC_4H_6^+$ ion has a VO^+-butadiene structure, while the $VOC_4H_8^+$ ion is a bis(ethene) species, as is shown by the CID spectra of the two species. $VOC_4H_6^+$ regenerates VO^+ as the primary CID product, while $VOC_4H_8^+$ produces predominately $VOC_2H_4^+$ at low CID energies and VO^+ at high energies. With cyclopentane, both single and double dehydrogenations are seen with VO^+, while V^+ produces only the double dehydrogenation product. The product ions formed with VO^+ do react further to form $VOC_{10}H_{12}^+$, the bis(cyclopentadiene) product, and only a trace of $VOC_{10}H_{10}^+$, while the V^+ products react to produce exclusively the bis(cyclopentadienyl) product. Cyclohexane undergoes one, two, and three dehydrogenations with VO^+, while V^+ induces a minimum of two. Finally, VO^+ produces, again, products corresponding to one, two, and three dehydrogenations with methylcyclohexane, in addition to formation of $VOC_6H_6^+$, while V^+ forms only $VC_7H_8^+$ and $VC_6H_6^+$. None of the product ions from VO^+ react further with cyclohexane or methylcyclohexane, while secondary reactions are observed with V^+, again suggesting that the presence of the oxygen ligand reduces the number of coordination sites, preventing further interactions.

Conclusions

The V^+ ion reacts with hydrocarbons primarily by insertion into C-H bonds inducing dehydrogenation. In contrast to some of the later first-row transition-metal ions, such as Fe^+, Co^+, and Ni^+,[2b] formation of secondary reaction products occurs with all of the hydrocarbons studied save for the largest linear alkanes.

Addition of an oxide ligand to V^+, producing VO^+, does not greatly change the chemistry observed. VO^+ does react somewhat slower than V^+ and is not as effective at dehydrogenating alkanes. In cases where coordinative saturation may influence reactivity, such as formation of secondary products, an effect is seen. In contrast to FeO^+,[4] the oxide ligand does not appear to be involved in the reactions of VO^+, since it is never lost in the course of reaction, and collision-induced dissociation of product ions containing VO^+ always results in reformation of VO^+ by loss of other ligands. This effect is undoubtedly due to the strong V^+-O bond.

Acknowledgment is made to the Division of Chemical Sciences in the office of Basic Energy Sciences in the United States Department of Energy (DE-AC02-80ER10689) and the National Science Foundation (CHE-8310039) for supporting the advancement of FTMS methodology. We also would like to thank Dr. D. B. Jacobson for helpful discussions.

Registry No. VO^+, 12192-26-6; V^+, 14782-33-3; CH_4, 74-82-8; C_2H_6, 74-84-0; propane, 74-98-6; butane, 106-97-8; pentane, 109-66-0; hexane, 110-54-3; heptane, 142-82-5; octane, 111-65-9; nonane, 111-84-2; 2-methylpropane, 75-28-5; 2-methylbutane, 78-78-4; 2,2-dimethylpropane, 463-82-1; 2,3-dimethylbutane, 79-29-8; 2,2-dimethylbutane, 75-83-2; 2,2,3,3-tetramethylbutane, 594-82-1; cyclopropane, 75-19-4; cyclobutane, 287-23-0; cyclopentane, 287-92-3; cyclohexane, 110-82-7; methylcyclohexane, 108-87-2.

Reactive Ion Pairs from the Charge-Transfer Excitation of Electron Donor-Acceptor Complexes

J. M. Masnovi,[1a] J. K. Kochi,*[1a] E. F. Hilinski,[1b] and P. M. Rentzepis*[1c]

Contribution from the Department of Chemistry, University of Houston, University Park, Houston, Texas 77004, and AT&T Bell Laboratories, Murray Hill, New Jersey 07974.
Received July 5, 1985

Abstract: Excitation within the charge-transfer (CT) band of the electron donor-acceptor or EDA complexes of tetranitromethane (TNM) with a series of 9-substituted and 9,10-disubstituted anthracenes (An) leads to photochemistry in high quantum yields ($\Phi \sim 1$). The combined use of time-resolved picosecond spectroscopy, product isolation, and structure elucidation allows for the detailed mapping of the temporal evolution of the CT excited state to the photoproduct I via a series of discrete reactive intermediates. Thus electron transfer within the EDA complex occurs effectively (<25 ps) upon CT photoexcitation to form simultaneously $An^{+\cdot}$ and $TNM^{-\cdot}$. The latter is not observed directly owing to its spontaneous fragmentation to $C(NO_2)_3^-$ and NO_2 within 10 ps. The geminate ionic intermediates $An^{+\cdot}$ and $C(NO_2)_3^-$ undergo cage combination to produce hydranthryl radicals II within an interval of <500 ps. Photoproduct I derives from the encounter of the hydranthryl radical II with NO_2 subsequent to diffusive separation, consistent with the longer time scale of >1 ns and the trans stereochemistry required for the free radical coupling to occur. This detailed study is the basis for a generalized formulation (summarized in Scheme I) to be developed for CT photochemistry via reactive ion pairs. In particular, the comparison with the related EDA complexes of the anthracenes and tetracyanoethylene serves to emphasize the importance of back electron transfer from the geminate ion pair, i.e., $[D^{+\cdot}, A^{-\cdot}] \rightarrow [D, A]$.

Electron donor-acceptor or EDA complexes are commonly found as intermediates in a wide variety of reactions involving electron-rich species or donors (D), such as nucleophiles and bases, and electron-deficient acceptors (A).[2] For example, the well-known electrophilic aromatic substitutions such as chlorination, bromination, mercuration, thallation, etc., involve the EDA complexes of arenes with the acceptors Cl_2, Br_2, Hg(II), and Tl(III), respectively.[3] Since charge-transfer (CT) interactions provide substantial stabilization of the transition states for such processes,[4] we have begun a thorough picosecond spectroscopic study of the photochemical behavior of the excited states of EDA complexes.[5]

(1) Present addresses: (a) J. M. Masnovi and J. K. Kochi, Department of Chemistry, University of Houston, University Park, Houston, Texas 77004. (b) E. F. Hilinski, Department of Chemistry, Florida State University, Tallahasee, Florida, 32306. (c) P. M. Rentzepis, AT&T Bell Laboratories, Murray Hill, New Jersey 07974.

(2) (a) Foster, R. "Organic Charge-Transfer Complexes"; Academic Press: New York, 1969. (b) Andrews, L. J.; Keefer, R. M. "Molecular Complexes in Organic Chemistry"; Holden Day: San Francisco, 1964. (c) Briegleb, G. "Elektronen-Donator-Acceptor Komplexe"; Springer Verlag: Berlin, 1961.

(3) (a) Fukuzumi, S.; Kochi, J. K. *J. Am. Chem. Soc.* **1981**, *103*, 7240. (b) Lau, W.; Kochi, J. K. *J. Am. Chem. Soc.* **1984**, *106*, 7100.

(4) Fukuzumi, S.; Kochi, J. K. *J. Am. Chem. Soc.* **1982**, *104*, 7599.

(5) (a) Hilinski, E. F.; Masnovi, J. M.; Amatore, C.; Kochi, J. K.; Rentzepis, P. M. *J. Am. Chem. Soc.* **1983**, *105*, 6167. (b) Hilinski, E. F.; Masnovi, J. M.; Kochi, J. K.; Rentzepis, P. M. *Ibid.* **1984**, *106*, 8071.

0002-7863/86/1508-1126$01.50/0

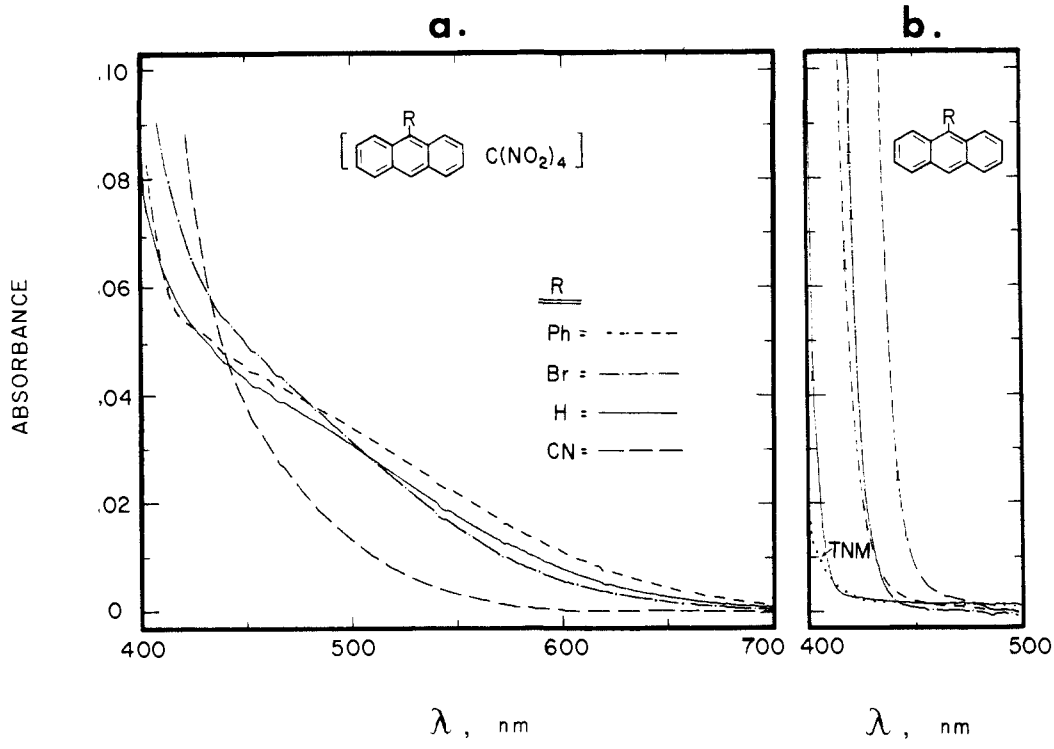

Figure 1. (a) CT absorption spectra of the EDA complexes of 0.02 M tetranitromethane with 0.02 M 9-phenylanthracene (---), anthracene (—), 9-cyanoanthracene (– –), and 9-bromoanthracene (-·-) in dichloromethane solutions with a 1-cm optical path. (b) The long-wavelength cutoffs of 0.02 M anthracene derivatives and tetranitromethane alone in the same solvent are included for comparison.

Aromatic donors readily form EDA complexes with various types of π-acceptors such as tetracyanoethylene (TCNE), chloranil, pyromellitic anhydride, etc., which are related to those formed with the electrophiles described above.[6] Our previous investigation of a series of 9-substituted and 9,10-disubstituted anthracenes (An) with TCNE established that the selective irradiation within the lowest energy CT absorption band leads directly to the geminate radical-ion pair,[5] i.e.

$$\underset{\text{EDA complex}}{\text{An + TCNE} \rightleftharpoons [\text{An, TCNE}]} \xrightarrow{h\nu_{CT}} [\text{An}^{+}\cdot, \text{TCNE}^{-}\cdot] \quad (1)$$

The observation of such an ion pair is consistent with the predictions of Mulliken theory[7] that the CT excitation of weakly associated EDA complexes results in the promotion of an electron from the highest occupied molecular orbital (HOMO) of the donor to the lowest unoccupied molecular orbital (LUMO) of the acceptor. It is important to emphasize that our experimental time resolution of <25 ps for the spectroscopic detection of transients ensures that excitation of the EDA complex generates a geminate ion pair. Such an ion pair is born with the mean separation between the donor and acceptor moieties which is approximately the same as that extant in the ground state of the EDA complex. In the TCNE system, the rate of the back electron transfer within the ion pair to regenerate the EDA complex is rapid, i.e.

$$[\text{An}^{+}\cdot, \text{TCNE}^{-}\cdot] \xrightarrow{<50\text{ ps}} [\text{An, TCNE}] \quad (2)$$

This is consistent with the observed quantum yield for photochemical reaction of essentially zero, and no products are formed irreversibly upon continuous irradiation of the CT absorption band.

We therefore sought an alternative system in which to study ion-pair photochemistry which is attendant upon the CT excitation of EDA complexes. Indeed tetranitromethane (TNM) is known to form EDA complexes with aromatic donors,[8,9] and efficient photochemistry has been observed in these and related complexes.[10,11] Accordingly in this report, we elucidate the CT photochemistry of the EDA complexes of TNM by focussing on the same series of 9-substituted and 9,10-disubstituted anthracenes which were previously examined with TCNE.[5]

Table I. Comparison of the EDA Complexes of Anthracene with TNM and TCNE[a]

9-substituted anthracene	acceptor	$K\epsilon$ (M^{-2} cm^{-1})	K (M^{-1})	ϵ (M^{-1} cm^{-1})
NO_2	TCNE	303	1.5	260[b]
CHO[c]	TCNE	1180	4.8	250[d]
CN	TNM	41	0.24	170[e]
H	TNM	93	0.31	300[e]
C_6H_5	TNM	110	0.62	180[e]

[a] In dichloromethane at 24 °C with the acceptor in excess. [b] Measured at λ_{max} 616 nm. [c] In chloroform, ref 13. [d] Measured at λ_{max} 668 nm. [e] Measured at 500 nm in the absorption tail. Differences probably reflect change in λ_{max} (which is obscured by local absorptions of the donor and acceptor).

Results

I. Charge-Transfer Spectra of Anthracene–TNM Complexes. When a colorless solution of tetranitromethane is mixed with that

(6) Fukuzumi, S.; Kochi, J. K. *J. Org. Chem.* **1981**, *46*, 4116.
(7) Mulliken, R. S. *J. Am. Chem. Soc.* **1952**, *74*, 811. Mulliken, R. S.; Person, W. B. "Molecular Complexes: A Lecture and Reprint Volume"; Wiley: New York, 1969.

(8) (a) Hammond, P. R.; Burkardt, L. A. *J. Phys. Chem.* **1970**, *74*, 639. (b) Lagercrantz, C.; Yhland, M. *Acta Chem. Scand.* **1962**, *16*, 1807. (c) Jaworska-Augustyniak, A. *Transition Met. Chem. (Weinheim, Ger.)* **1981**, *6*, 100. (d) Le Fevre, R. J. W.; Radford, D. W.; Stiles, S. J. *J. Chem. Soc. B* **1968**, 1297. (e) Kholmogrov, V. E.; Gorodyskii, V. A. *Zh. Fiz. Khim.* **1972**, *46*, 63.
(9) (a) Newman, M. S.; Le Blanc, J. R.; Karnes, H. A.; Axelrod, G. *J. Am. Chem. Soc.* **1964**, *86*, 868. (b) Chaudhuri, J. N.; Basu, S. *J. Chem. Soc.* **1959**, 3085. (c) Gorodyskii, V. A.; Pozdnyakov, V. P.; Siretskii, Ye. G.; Fadeeva, I. I.; Kozlov, L. P. *Zh. Fiz. Khim.* **1974**, *48*, 2190. Gorodyskii, V. A.; Siretskii, Yu. G.; Fadeeva, I. I.; Kozlov, L. P. *Ibid.* **1974**, *48*, 801.
(10) (a) Seltzer, S.; Lam, E.; Packer, L. *J. Am. Chem. Soc.* **1982**, *103*, 6470. (b) Penczek, S.; Jagur-Grodzinski, J.; Szwarc, M. *Ibid.* **1968**, *90*, 2174. Grumbs, R.; Penczek, S.; Jagur-Grodzinski, J.; Szwarc, M. *Macromolecules* **1969**, *2*, 77. (c) Isaacs, N. S.; Abed, O. H. *Tetrahedron Lett.* **1982**, *23*, 2799. (d) Iles, D. H.; Ledwith, A. *J. Chem. Soc., Chem. Commun.* **1969**, *364*. (e) Leenson, I. A.; Sergeev, G. B. *Khim. Vys. Energ.* **1971**, *5*, 370.
(11) For a preliminary account of this work see: Masnovi, J. M.; Huffman, J. C.; Kochi, J. K.; Hilinski, E. F.; Rentzepis, P. M. *Chem. Phys. Lett.* **1984**, *106*, 20.

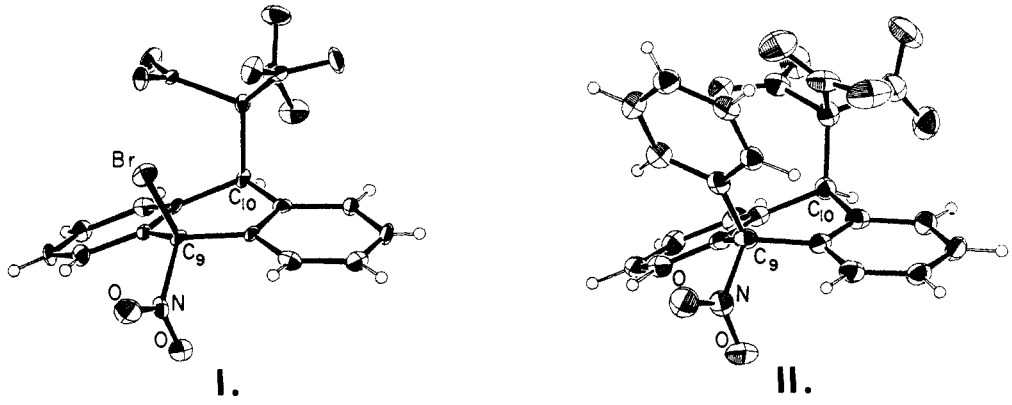

Figure 2. ORTEP drawings of the molecular structures of the photoproduct I derived from the CT excitation of the EDA complex of (left) 9-bromoanthracene and (right) 9-phenylanthracene in methylene chloride.

of a 9-substituted anthracene (An), the brown color of the EDA complex is immediately apparent. These complexes persist in methylene chloride solutions for many hours at room temperature if the solutions are carefully shielded from light. The charge-transfer spectra of the EDA complexes appear as broad absorption bands to lower energy from the localized transitions of either the anthracene donor or TNM, as illustrated in Figure 1, a and b, respectively. The CT absorption bands of these anthracene complexes with TNM differ from the corresponding TCNE complexes examined earlier by being blue-shifted ($\Delta\lambda \geq 300$ nm) and showing significantly broader bandwidths (compare Figure 1 with Figure 1 in ref 5b).

II. Association Constants for Anthracene–TNM Complexes. Comparison with TCNE Complexes. The association constants for the EDA complexes of TNM and TCNE with the representative anthracenes listed in Table I were determined by the Benesi–Hildebrand (B–H) method.[2a]

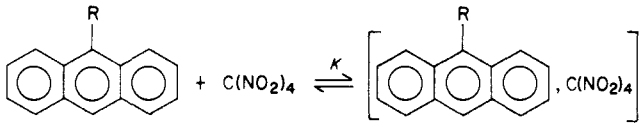

(3)

The value of the association constant K was obtained from the slope of the B–H plot by using the extrapolated value of the extinction coefficient ϵ at the intercept and assuming the formation of 1:1 complexes (see Experimental Section). To avoid complications arising from higher order complexes,[12] all measurements were carried out with the acceptor in excess. The magnitudes of K for complex formation are rather small for both TCNE and TNM acceptors, although the latter are consistently weaker by about an order of magnitude. Thus both series of EDA complexes are considered to be weakly bound. They are not easily differentiated on the basis of the magnitude of the CT transition moments (see column 5, Table I).

III. Photoproducts Derived from the CT Excitation of Anthracene–TNM Complexes. The absorption spectra in Figure 1 assure us that the incident light is absorbed exclusively by the EDA complex at $\lambda > 480$ nm. Thus we were able to examine the CT photochemistry by irradiating an equimolar (0.1 M) solution of the anthracene and TNM in methylene chloride with a focussed beam from a 500-W xenon lamp passed through glass filters with sharp cutoffs at either 500 or 560 nm (Corning No. 3-69 or 2-63). The course of photochemistry was readily followed by the bleaching of the CT absorption band, and it was generally complete within 15 min.

The ^{1}H NMR spectrum of the photolyzed solution was always characterized by the appearance of an unusually broadened singlet resonance in the region between δ 6.0 and 6.7. The singlet resonance sharpened at low temperatures and broadened (reversibly) as the temperature was increased. This unique behavior of the singlet resonance proved to be an invaluable diagnostic tool for following the course of photochemistry.

Table II. Quantum Yields for the Disappearance of the EDA Complex from Anthracenes with TNM and the Appearance of Photoadduct I[a]

9-substituted anthracene	Φ_{-CT}	Φ_{-An}	Φ_P
NO_2	1.5	0.7	0.6
CHO	1.61		
H	1.62	0.75	0.3
	0.73[b]		
C_6H_5	1.5	0.6	0.4

[a] In methylene chloride solution containing 0.050 M An and 0.050 M TNM at 25 °C. [b] With 0.050 M An and 0.50 M TNM.

The principal photoproducts I, particularly those derived from anthracenes bearing electron-withdrawing substituents at the 9-position, were usually isolated in good yields by fractional crystallization. In particular, we successfully grew single crystals of the photoproducts I derived from 9-bromo and 9-phenyl derivatives, and their molecular structures were established by X-ray crystallography. The ORTEP diagrams presented in Figure 2 show the principal photoproduct I to be a 1:1 adduct in which the TNM fragments, $C(NO_2)_3^-$ and NO_2, have simply added to the meso positions of the anthracene with trans stereochemistry. The central cyclohexadiene ring is boat-shaped with the large trinitromethyl group always situated pseudoaxially at the 10-position. [A preference for the bulkier substituent on 9,10-dihydroanthracenes to occupy pseudoaxial positions has been noted in other derivatives.[14]] We assign the characteristic singlet resonance in the ^{1}H NMR spectrum to the equatorial proton at the 10-position of I and account for the temperature-dependent line broadening of this singlet to restricted conformational motions of the axial $C(NO_2)_3$ substituent at the same carbon center. (See Figure 2 for the steric constraints). By way of comparison, the photoadduct I derived from TNM and anthracene itself showed two singlet resonances arising from a pair of protons at the meso or 9- and 10-positions. The former at δ 6.41 remained sharp, whereas the latter at δ 6.26 showed marked broadening between 25 and −60 °C. We used this characteristic temperature-dependent line-broadening to assign the regiochemistry of the photoaddition to all the 9-R-substituted anthracenes as that given in structure I, viz., 9-R-9-nitro-10-trinitromethyl-9,10-dihydroanthracene.[15]

IV. Quantum Yields for CT Photochemistry of Anthracene–TNM Complexes. The quantum yield for the photochemistry of the anthracene–TNM complexes was determined by two independent measurements involving the disappearance of the ab-

(12) Masnovi, J. M.; Hilinski, E. F.; Rentzepis, P. M.; Kochi, J. K. *J. Phys. Chem.* **1985**, *89*, 5387.

(13) Figeys, H. P.; Wilmet-Devos, B. *Bull. Soc. Chim. Belg.* **1970**, *79*, 459.

(14) (a) Cam, W.; Bock, H. *Chem. Ber.* **1978**, *111*, 3585. (b) Dalling, D. K.; Zilm, K. W.; Grant, D. M.; Heeschen, W. A.; Horton, W. J.; Pugmire, R. J. *J. Am. Chem. Soc.* **1981**, *103*, 4817.

(15) For structure assignment, see: Masnovi, J. M.; Kochi, J. K. *J. Org. Chem.*, in press.

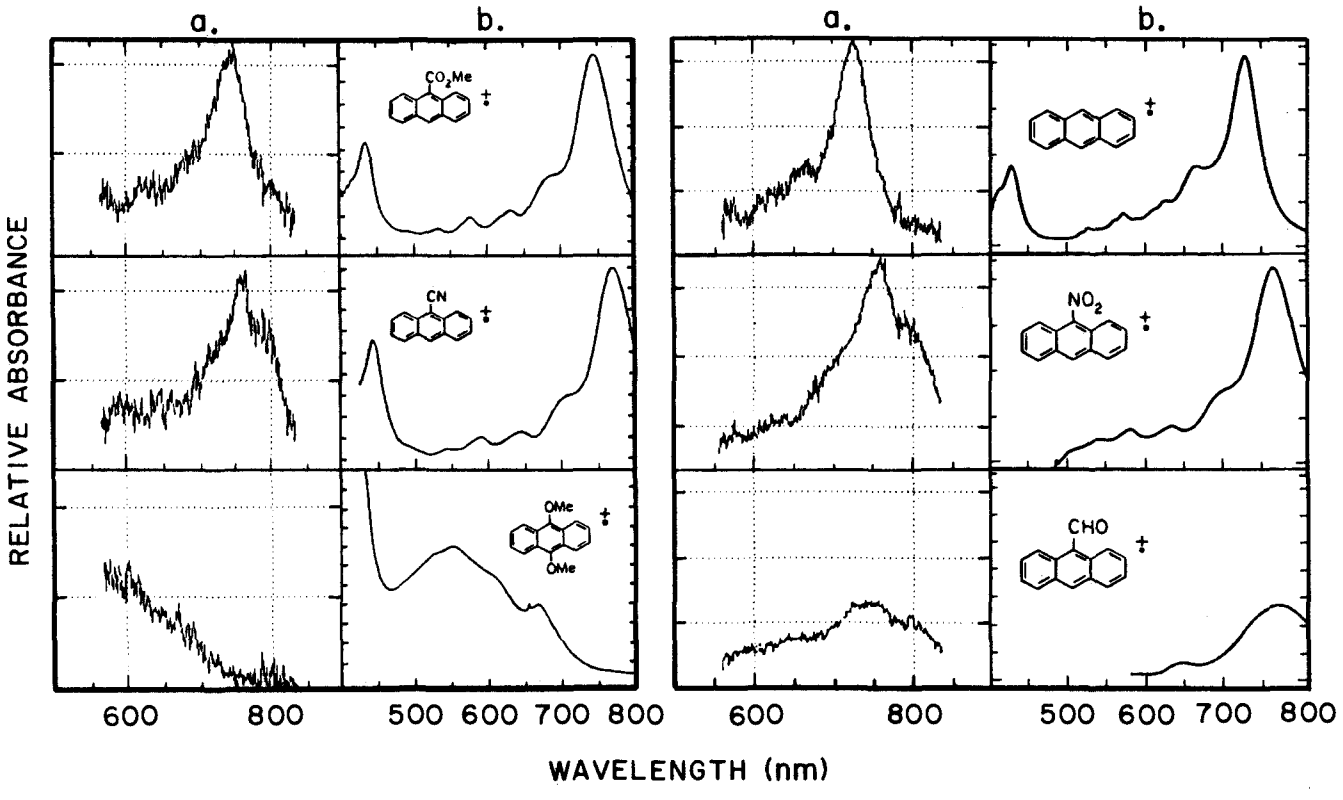

Figure 3. (a) Transient absorption spectra of arene cation radicals derived from 9-nitroanthracene, 9-formylanthracene, 9-carbomethoxyanthracene, anthracene, 9-cyanoanthracene, and 9,10-dimethoxyanthracene recorded 25 ps after 532-nm excitation of the respective EDA complex with tetranitromethane in dichloromethane. (b) Absorption spectra of the corresponding anthracene cation radicals generated by anodic oxidation.

sorption band of the EDA complex ($\Phi_{\text{-CT}}$) as well as that of the anthracene donor ($\Phi_{\text{-An}}$) to low conversions (<10%). The results presented in Table II show that $\Phi_{\text{-CT}} = \Phi_{\text{-An}}$ when TNM is in 10-fold excess; and $\Phi_{\text{-CT}} \sim 2\Phi_{\text{-An}}$ when equimolar amounts of the anthracene and TNM were present. This result is consistent with the consumption of the donor and the acceptor in equal amounts directly from the 1:1 EDA complexe, i.e.

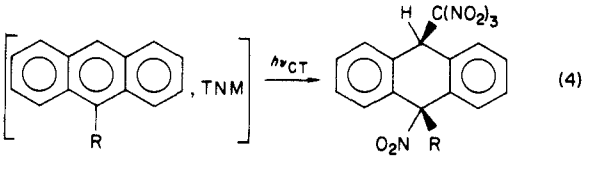

(4)

under conditions in which complex formation (i.e., K) is limited.[16] [The disappearance of TNM could not be monitored directly.] The quantum yield Φ_P for the formation of the photoadducts I is indicated in Table II by the values listed in column 4 which were obtained by multiplying $\Phi_{\text{-An}}$ by the yields of the photoproduct I.

V. Spectral Observation of Reactive Intermediates by Time-Resolved Picosecond Spectroscopy. The events following the CT excitation of EDA complexes were examined by transient picosecond absorption techniques.[17] The excitation was carried out either at 266 or 532 nm with a single 25-ps (fwhm) laser pulse (~ 1 mJ).

Anthracene Cation Radicals. The difference absorption spectra measured at 25 ps after the 532-nm excitation are shown in Figure 3a for the TNM complexes of representative 9-substituted and 9,10-disubstituted anthracenes in methylene chloride solution. The intense transient absorption bands with maxima between 720 and 780 nm are formed within the 25-ps laser pulse. These absorption bands are assigned to the radical cations ($An^{+}\cdot$) of the respective anthracene donors based on comparisons with the spectra (Figure 3b) of radical cations generated by anodic oxidation.[18] It is singularly noteworthy that these transient absorption spectra of $An^{+}\cdot$ are essentially the same as those previously observed in the time-resolved picosecond studies of the anthracene–TCNE complexes.[5] The observation further confirms the photodissociation of the EDA complexes to two very weakly coupled ion radicals.

Trinitromethide Anion. The intense absorptions of the anthracene donors obscure the spectral region below 450 nm (See Figure 1b). In order to survey this spectral region, we turned to the complexes of TNM with hexamethylbenzene (HMB) and hexaethylbenzene (HEB) because these donors absorb at wavelengths lower than 300 nm. The sequence of time-resolved spectra taken at 25-ps intervals following the 266-nm excitation of solutions of HMB and TNM is shown in Figure 4a. Two transient absorption bands appeared within the 25-ps laser pulse. One band system, centered near 500 nm, is assigned to the hexamethylbenzene radical cation $HMB^{+}\cdot$ by comparison with the absorption spectrum shown in Figure 4b which was obtained from the electrochemical oxidation of hexamethylbenzene.[19] The second transient absorption band appears at ~350 nm (Figure 4a), and it is assigned to the known trinitromethide anion $C(NO_2)_3^{-}$ which can be prepared by either the cathodic or chemical reduction of TNM (Figure 4b).[20,21] Neither of these transients are observed when either the arene donor or TNM is irradiated alone. No other absorptions, such as those ascribable to an excited state of an EDA complex or to the putative acceptor anion $TNM^{-}\cdot$, are discernible. The same results were obtained from the CT irradiation of the EDA complex of hexaethylbenzene and tetranitromethane.

The spectrum of nitrogen dioxide consists of a weak, broad continuum spanning the spectral range of 250 nm to longer than

(16) At low conversions the concentration of the EDA complex diminishes roughly twice as fast as either [D] or [A] when K is small and [D] = [A], i.e., $\Delta[EDA] \approx 2\Delta D = 2\Delta A$, since each photochemical event destroys 1D and 1TNM. Therefore $\Phi_{\text{-CT}} \approx 2\Phi_{\text{-D}} = 2\Phi_P$.

(17) Hilinski, E. F.; Rentzepis, P. M. *Anal. Chem.* **1983**, *55*, 1121A.

(18) Masnovi, J. M.; Seddon, E. A.; Kochi, J. K. *Can. J. Chem.* **1984**, *62*, 2552.

(19) Cf.: Peacock, N. J.; Schuster, G. B. *J. Am. Chem. Soc.* **1983**, *105*, 3632, ref 3b and 18.

(20) Glover, D. J. *Tetrahedron* **1963**, *19* (Suppl. 1), 219. Kamlet, M. J.; Glover, D. J. *J. Org. Chem.* **1962**, *27*, 537.

(21) Young, R. P.; Holt, A.; Walker, S. *Tetrahedron* **1964**, *20*, 2351.

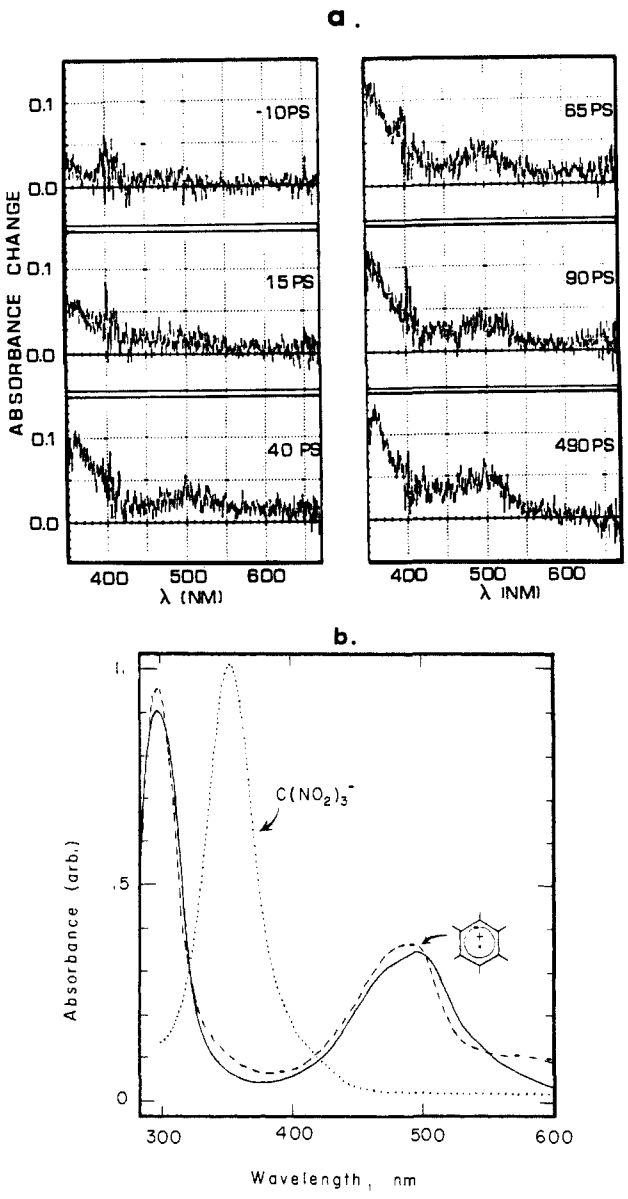

Figure 4. (a) Difference absorption spectra obtained from the irradiation with a 266-nm, 25-ps laser pulse of a solution of 0.1 M hexamethylbenzene and 0.1 M TNM in methylene chloride taken at −10, 15, 40, 65, 90, and 490 ps. (b) Absorption spectra of hexamethylbenzene (---) and hexaethylbenzene (—) cation radicals and trinitromethide anion (···) generated by the electrochemical oxidation of arene and reduction of TNM, respectively, in CH_2Cl_2 containing 0.1 M tetrabutylammonium perchlorate.

800 nm.[22] We have been unable to confirm directly its formation; however, we believe NO_2 contributes to the absorption bands observed in the transient spectra, although its spectrum is obscured by the more intense bands arising from other transients. In particular, the presence of NO_2 may be surmised as a weak residual absorption at longer times (nanoseconds) following excitation.

Hydranthryl Radicals. We observe that during the interval between 50 ps and 4 ns after excitation, the absorption intensity of the anthracene radical-cation band largely decays. The growth of a new absorption band centered near 500 nm is consistent with the decay of $An^{+}\cdot$. This is particularly evident in the spectral changes for the 9-nitroanthracene complex with TNM in Figure 5a. A similar new absorption was also observed with 9-cyanoanthracene and TNM, as shown by a comparison of the 10- and 2000-ps spectra in Figure 6. We assign this absorption band, which persists for longer than 4 ns, to the adduct radical II derived from the reaction of $An^{+}\cdot$ with trinitromethide, i.e.

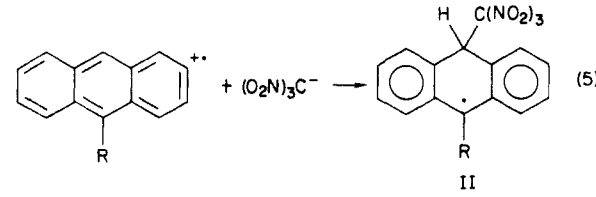

This assignment of 9-substituted-10-trinitromethyl-10-hydranthryl radical is based on the independent spectroscopic observation of the related 9-cyano-10-hydranthryl radical generated from 9-cyanoanthracene during pulse radiolysis in ethanol.[23]

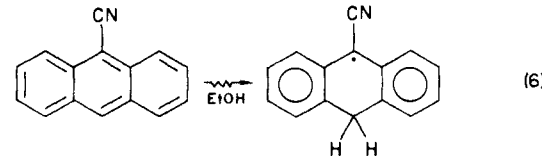

Absorption bands in the spectral region near 550 nm are also characteristic of the related diarylmethyl and triarylmethyl radicals.[24]

VI. The Decay of the Reactive Radical-Ion Pairs. The sequence of spectral changes following the CT excitation of the TNM complexes of (a) 9-nitroanthracene, (b) anthracene, and (c) 9-formylanthracene is shown in Figure 5. The time-resolved spectra in the region between 550 and 800 nm reveals (a) the disappearance of the anthracene cation radical at ~750 nm and (b) the growth of the hydranthryl radical at ~550 nm (vide supra).

The rate of disappearance of $An^{+}\cdot$ is clearly seen to be highly dependent on the anthracene donors—those with electron-withdrawing substituents (R = NO_2, CHO) decaying within ~500 ps whereas anthracene cation radical itself persists beyond 4 ns. If we focus on the time interval less than 500 ps, the decay of $An^{+}\cdot$ will largely reflect first-order processes arising from geminate species, with minimal complications from diffusion. Accordingly, the first-order rate constants were extracted from the time-resolved spectra in Figure 5. They are estimated to be 1.5×10^9, 3.2×10^9, and 3.3×10^9 s^{-1} when R = H, NO_2, and CHO, respectively.

The growth of the hydranthryl radical II (which is particularly apparent in Figure 5a) occurs with about the same rate as $An^{+}\cdot$ decays. This observation is consistent with the cage combination of the ion pair according to the stoichiometry described in eq 5. If so, we estimate from the relative change in the absorbances in Figure 5 that the extinction coefficient of the 9-nitrohydranthryl radical II at 550 nm is roughly 15–20% as large as the extinction coefficient of the $An^{+}\cdot$ precursor at λ_{max} 757 nm.[25] Weak (continuous) absorptions which extend beyond 800 nm are evident as background at long times (ns) after CT excitation. These more persistent absorptions are consistent with those arising from nitrogen dioxide which combines with the hydranthryl radical at longer times to generate photoproduct I.

Discussion

The electron donor–acceptor complexes of anthracenes with tetranitromethane and tetracyanoethylene offer an ideal system in which to examine the photophysics of the charge-transfer excitation and the attendant photochemistry. In this system, the CT absorption bands are sufficiently prominent and well separated from the absorption bands of either the donor (D) or the acceptor (A). Thus there is no ambiguity about either the adventitious local excitation of complexed or uncomplexed chromophores or

(22) (a) Hall, Jr.; Blacet, F. E. *J. Chem. Phys.* **1952**, *20*, 1745. (b) Gillispie, G. D.; Khan, A. V. *Ibid.* **1976**, *65*, 1624 and references therein.

(23) Okada, T.; Kida, K.; Mataga, N. *Chem. Phys. Lett.* **1982**, *88*, 157.

(24) (a) Chu, T. L.; Weissman, S. I. *J. Chem. Phys.* **1954**, *22*, 21. (b) Gallinga, G.; Mackor, E. L.; Stuart, A. A. V. *Mol. Phys.* **1958**, *1*, 123. (c) Kerimov, O. M.; Maksyutov, E. M.; Milonich, A. I.; Slovetskii, V. I. *Izv. Akad. Nauk SSR* **1979**, 623 and references therein.

(25) For anthracene cation radical ϵ_{max} 7700 M^{-1} cm^{-1}. See: Torikai, A.; Kato, R. *J. Polym. Sci.: Poly. Chem. Ed.* **1978**, *16*, 1487.

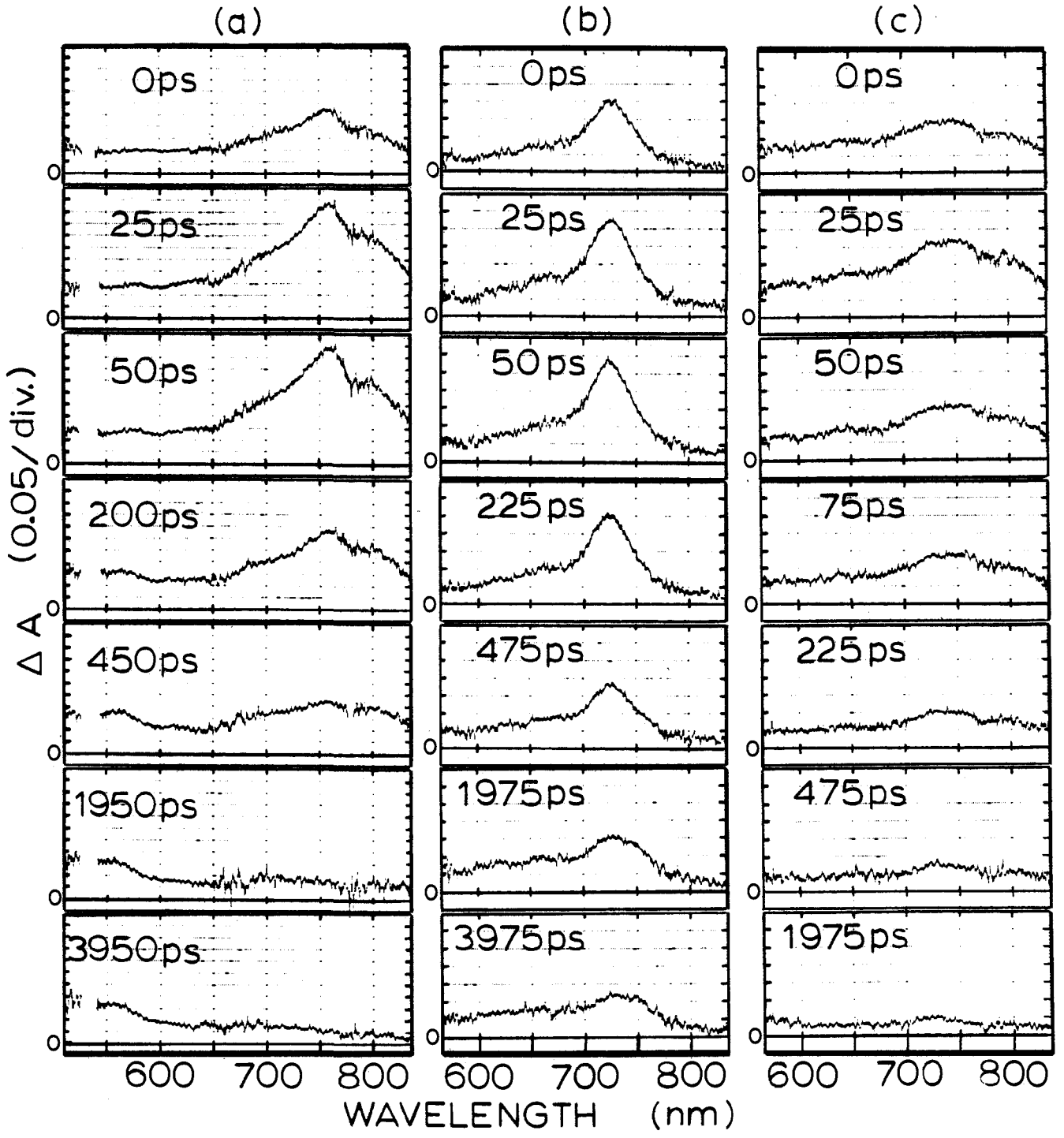

Figure 5. Time-resolved picosecond absorption spectra following 532-nm excitation of the EDA complexes of equimolar tetranitromethane with (a) 0.2 M 9-nitroanthracene, (b) 0.1 M anthracene, and (c) 0.1 M 9-formylanthracene in dichloromethane.

the generation of intermediates which do not result from the CT excitation of the EDA complex.

The time-resolved picosecond spectra in Figures 3 and 5 demonstrate that electron transfer within the EDA complexes of arene donors and TNM effectively occurs upon absorption of a photon. These studies show unequivocally that our proposal[5] for the production of ion pairs from the selective excitation of the charge-transfer band is correct, and in agreement with the Mulliken model for electron transfer upon photoexcitation of the EDA complex, i.e.

$$D + A \rightleftharpoons [D, A] \xrightarrow{h\nu_{CT}} [D^{+}\cdot, A^{-}\cdot] \qquad (7)$$

As similar as the CT excitation of TCNE and TNM complexes are, however, they differ markedly in the fates of their excited ion pairs. On one hand, the ion pair derived from TCNE undergoes rapid back electron transfer within ~50 ps to restore the EDA complex, i.e.

$$[An^{+}\cdot, TCNE^{-}\cdot] \xrightarrow{<50\ ps} [An, TCNE]$$

In contrast, the geminate ion pair from TNM decays by a process that efficiently generates photoproducts such as the meso adduct I, since the quantum yields for the disappearance of the donor is greater than 0.7. Thus back electron transfer within the geminate ion pair can account for no more than 20–30% of the deactivation process. Indeed the rate of chemical evolution following the CT excitation of TNM complexes can be estimated to be $\geq 2 \times 10^{11}$ s^{-1} if the rate of back electron transfer from the TNM ion pair is assumed to be the same as that ($\sim 7 \times 10^{10}$ s^{-1}) determined previously for the TCNE ion pair. Since the anthracene cation radicals $An^{+}\cdot$ derived from the complex with TNM

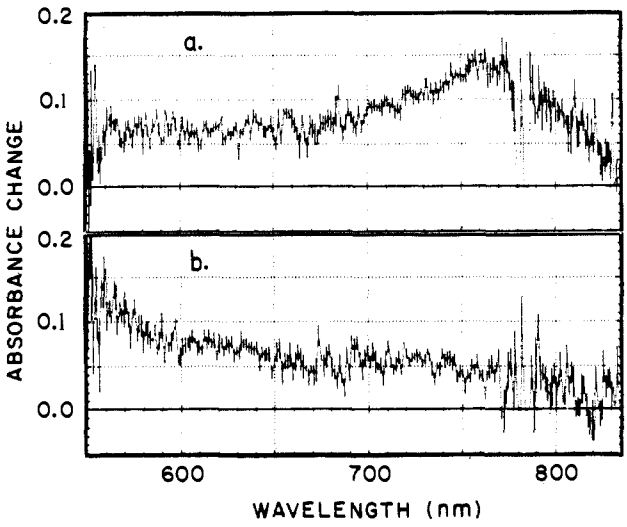

Figure 6. Time-resolved picosecond absorption spectra taken at (a) 10 ps and (b) 1985 ps following the 532-nm excitation of the EDA complexed derived from 0.2 M TNM and 0.2 M 9-cyanoanthracene in CH_2Cl_2.

are consistently longer lived than the same cation radicals derived from the complex with TCNE, the difference must lie with the radical anion. In particular, tetracyanoethylene undergoes reversible electron transfer and forms stable salts of $TCNE^{-}\cdot$.[26]

$$(NC)_2C{=}C(CN)_2 \overset{+e}{\rightleftharpoons} (NC)_2C{=}C(CN)_2^{-}\cdot \qquad (8)$$

By way of contrast, the tetranitromethane anion radical is unknown because it dissociates immediately upon electron capture. This is supported by pulse radiolysis studies,[27] i.e.

$$C(NO_2)_4 + e \rightarrow C(NO_2)_3^{-} + \dot{N}O_2 \qquad (9)$$

We independently confirmed the rapid fragmentation accompanying electron attachment to TNM in Figure 4. Thus the simultaneous appearance of the arene cation radical and $C(NO_2)_3^{-}$ within the rise time of the laser pulse demonstrates that the dissociative electron attachment to TNM occurs in less than 10 ps following CT excitation.

$$C(NO_2)_4 \xrightarrow{+e} C(NO_2)_4^{-}\cdot \xrightarrow{<10ps} C(NO_2)_3^{-} + \dot{N}O_2 \qquad (10)$$

If this fragmentation is responsible for the general photoreactivity of the EDA complexes of TNM, an upper limit of ~3 ps can be placed on the half-life of the TNM anion radical in the geminate radical ion pair,[28] i.e.

$$[An, C(NO_2)_4] \xrightarrow{h\nu_{CT}} [An^{+}\cdot, C(NO_2)_4^{-}\cdot] \xrightarrow{<3\ ps} [An^{+}\cdot, C(NO_2)_3^{-}, \dot{N}O_2] \qquad (11)$$

solvent-caged species

Such a short-lived species should be directly observable by time-resolved spectroscopy utilizing a shorter laser pulse.[29] It may answer the question of whether $TNM^{-}\cdot$ is a bound state or electron capture by TNM causes immediate dissociation.

The sequence of time-resolved spectral changes within the time interval of ~500 ps following CT excitation in Figure 5 illustrates the cage collapse of the geminate ion pair in eq 12 to the hydranthryl radical II.

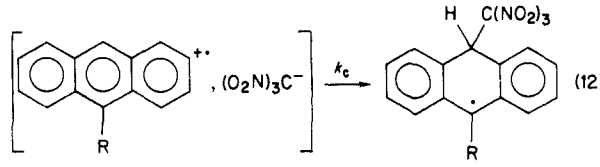

(12)

The rate of this geminate combination is highly dependent on the substituent R—the nitro and formyl derivatives being substantially more reactive than anthracene itself in accord with their more electron-deficient character. From the intensity measurements we deduce that cage combination as in eq 12 is the primary route by which the geminate ion pairs from the nitro and formyl derivatives react. The slower rate of cage combination of the anthracene cation radical with $C(NO_2)_3^{-}$, as indicated by the data in Figure 5b, allows a significant competition from the diffusive separation of the ions to occur, i.e.

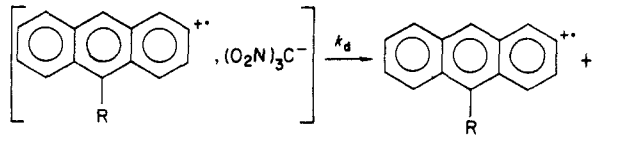

(13)

The residual absorption around 750 nm at longer times (>1 ns) must then arise from the separated cation radicals.[30] Indeed electron-rich anthracene derivatives such as that with a 9-phenyl substituent produce cation radicals which persist for prolonged periods following CT excitation. In this situation the combination of the geminate ion pairs is clearly not competitive with diffusive separation.

In 9-substituted anthracenes, the combination of the ion pair always occurs at the 10-position. This regiochemistry corresponds to the addition of the trinitromethide anion to the anthracene cation radical at the less hindered site in eq 12 in order to favor the more stable hydranthryl radical adduct.[31] Such a high regiospecificity in ion-pair collapse thus differs from the usual trends between reactivity and selectivity which have been observed in other bimolecular processes.[32]

The final stage of the photochemistry derives from the interaction of the adduct radical II with nitrogen dioxide to produce the ultimate photoproduct I with an overall high quantum yield, i.e.

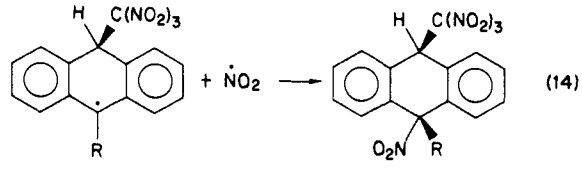

(14)

(26) (a) Webster, O. W.; Mahler, W.; Benson, R. E. *J. Am. Chem. Soc.* **1962**, *84*, 3678. (b) Itoh, M. *Ibid.* **1970**, *92*, 886. Itoh, M. *Bull. Chem. Soc. Jpn.* **1972**, *45*, 1947.

(27) (a) Rabani, J.; Mulac, W. A.; Matheson, M. S. *J. Phys. Chem.* **1965**, *69*, 53. (b) Chaudhri, S. A.; Asmus, K. D. *Ibid.* **1972**, *76*, 26.

(28) (a) For the rate of back-electron transfer of $k_{-et} \geq 7 \times 10^{10}\ s^{-1}$ (see ref 5), the rate of chemical evolution (τ^{-1}) $\simeq 3k_{-et} \geq 2 \times 10^{11}\ s^{-1}$ since $\Phi_{TNM} = \tau^{-1}/(\tau^{-1} + k_{-et}) \simeq 0.75$. In other words, the lifetime τ of $TNM^{-}\cdot$ is $\lesssim 5$ ps, or $t_{1/2} \lesssim 3$ ps. (b) The oxidation potential of $C(NO_2)_3^{-}$ has been reported as 1.95 V vs. SCE in acetonitrile [Kokorakina, V. A.; Feoktistov, L. G.; Shevelev, S. A.; Fainzil'berg, A. A. *Electrokhimiya* **1970**, 6, 1849.] Since the oxidation potentials of anthracenes are in the range $E^{\circ} \simeq 1.6$ V,[18] back-electron transfer from the ion pair $[An^{+}\cdot C(NO_2)_3^{-}]$ is thermodynamically unfavorable. The reformation of the reactants by an electron-transfer induced fragmentation of TNM is thus unlikely.

(29) Nitroalkanes afford stable anion radicals. [See: Saveant, J. M.; Tessier, D. *J. Phys. Chem.* **1977**, *81*, 2191.] A comparison of their electronic spectra suggests that the spectrum of $TNM^{-}\cdot$ may be red-shifted relative to that of TNM.

(30) Note in the anthracene system, we are unable to detect a measurable spectral shift of $An^{+}\cdot$ in the geminate ion pair compared to the free ion (see Figure 3). Compare: Simons, J. D.; Peters, K. S. *Acc. Chem. Res.* **1984**, *17*, 277. (b) We estimate that ~40% of anthracene radical-cation undergoes cage escape on the basis of the absorbance change at 50 ps relative to that at ~4 ns. The 9-nitro and 9-formyl derivatives suffer less (~5%) cage escape.

(31) (a) Replacement of a hydrogen by substituents usually leads to radical stabilization. See: O'Neal, H. E.; Benson, S. W. In "Free Radicals"; Kochi, J. K., Ed.; Wiley Interscience: New York, 1973; Vol. II, 275 ff. (b) For additions to the meso positions of anthracenes, see: Ito, Y.; Matsuura, A.; Otani, R.; Matsuura, T. *J. Am. Chem. Soc.* **1983**, *105*, 5699. Kiselev, V. D.; Miller, J. G. *Ibid.* **1975**, *97*, 4036. Yang, N. C.; Srinivasachar, K.; Kim, B.; Libman, J. *Ibid.* **1975**, *97*, 5006. Testaferri, L.; Tingoli, M.; Tiecco, M. *J. Chem. Soc., Perkin Trans. 2* **1983**, *543*.

(32) See Pross and Arnett and Reich [Pross, A. *Adv. Phys. Org. Chem.* **1977**, *14*. Arnett, E. M.; Reich, R. *J. Am. Chem. Soc.* **1978**, *100*, 2930] for a discussion of the reactivity–selectivity principle.

Scheme I. Charge-Transfer Photochemistry of Anthracene–TNM Complexes

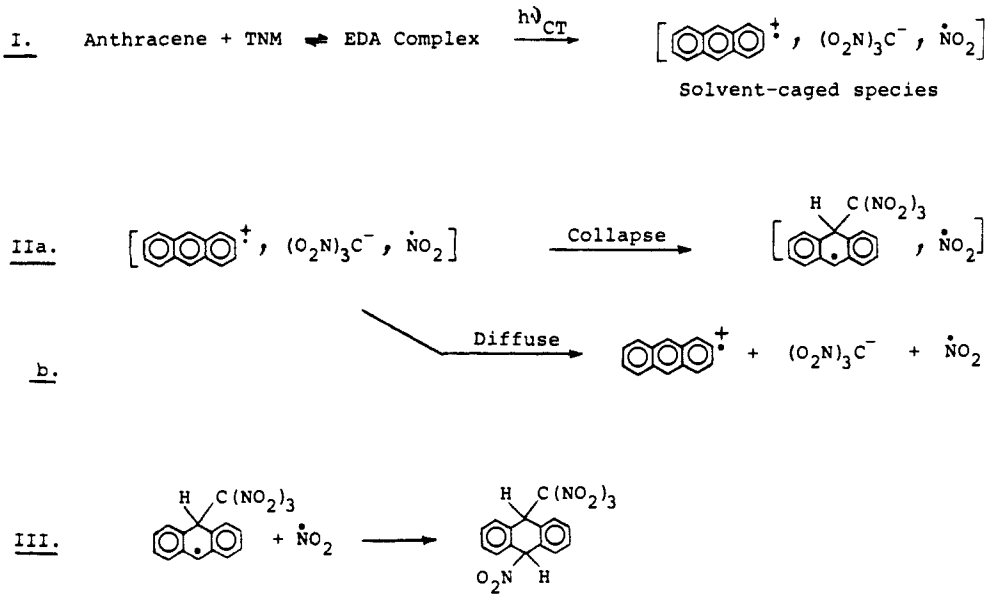

The molecular structures of the photoadducts **I** derived from the 9-bromo and 9-phenylanthracene indicate that NO_2 adds to the hydranthryl radical I from the side opposite the trinitromethyl substituent.[33]

Summary and Conclusions

We have applied conventional photochemistry, product isolation (structure determination), and time-resolved spectroscopy to successfully elucidate in detail the mechanism for the charge-transfer photochemistry of the EDA complexes derived from various anthracenes with tetranitromethane. The formation of the photoadduct I in high yields can be identified through the 3 discrete stages outlined in Scheme I.

The *first stage* represents the reversible, thermal association of the anthracene donor with the TNM acceptor to form the EDA complex (Figure 1 and Table I). Specific excitation of the charge-transfer band results in electron transfer within the complex to produce directly the anthracene cation radical $An^{+}\cdot$ within 25 ps (Figure 3). The anionic counterpart $TNM^{-}\cdot$ could not be observed spectroscopically owing to its spontaneous fragmentation to $C(NO_2)_3^-$ and NO_2 within 10 ps (Figure 4). The time scale of <25 ps for the spectral observation of these transients suggests that they all coexist as solvent-caged species depicted in brackets.

The *second stage* (<500 ps) corresponds to the cage combination of the geminate ion pair to generate hydranthryl radical adducts II in competition with the diffusive separation of the fragments (Figures 5 and 6). The formation of radical II is promoted by electron-withdrawing substituents on the anthracene, and it occurs at the unsubstituted meso position to produce the more stable 9-substituted-10-trinitromethyl-10-hydranthryl isomer.

The *last stage* (>1 ns) represents the interaction of the hydranthryl radical II with NO_2 to form the photoproduct I in high overall yields. The longer time intervals observed for this process, together with the stereochemical trans addition (Figure 2), indicate that the free-radical coupling involves diffusive encounters of II and NO_2 subsequent to separation of the caged species. This timing for the sequence of chemical events following CT excitation is supported by preliminary studies of the EDA complex immobilized in a glassy matrix.[34] The charge-transfer absorption spectrum (a) of 9-phenylanthracene and TNM in a methylcyclohexane glass at 77 K is shown in Figure 7. Irradiation of

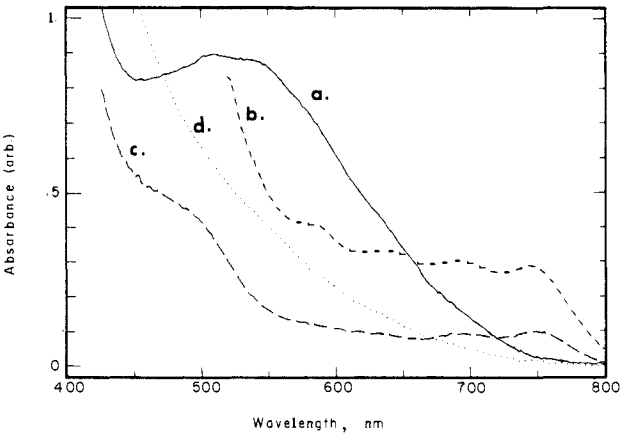

Figure 7. Difference absorption spectra in a glassy matrix: a (—) EDA complex of ~0.005 M 9-phenylanthracene and 0.10 M TNM in methylcyclohexane glass at 77 K; b (- - -) after brief irradiation of a at 77 K with irradiation $\lambda > 460$ nm; c (– –) after softening of the glass in b at 100 K; d (···) allowing the glass in c to thaw at 180 K in the dark.

this yellow-brown glass at 77 K with filtered light (cutoff at $\lambda < 460$ nm) results in a blue colored glass (b). The spectrum b consists of broad absorptions including a band with a maximum at ~750 nm characteristic of an anthracene cation radical absorption. The blue glass appears to be persistent indefinitely if kept in the dark at low temperatures.[35] Its ESR spectrum is composed of a broad unresolved signal. [In a related study carried out in an ethereal matrix at 77 K, Kholmogorov and Gorodyskii previously observed the ESR spectrum of NO_2 and an unresolved absorption assigned to $An^{+}\cdot$ on the basis of its optical absorption.[36]] Upon softening the glass at about 100 K, the blue color fades to the spectrum c showing an absorption at ~500 nm which we assign to the hydranthryl radical II. Only a nondescript tail absorption and no ESR signal remain when the glass is thawed at ~180 K. These matrix results thus agree with the time-resolved spectroscopic studies carried out in solution at 25 °C. Upon thawing the glass slowly, the photoadduct I is formed as the only isomer, albeit in reduced yields of 20–30%. The latter suggests the operation of the same mechanism following the CT excitation in Scheme I.

Finally, it is important to emphasize that despite the apparently disparate photochemical behavior of the TCNE and the TNM

(33) For the possibility of bridging in the hydranthryl radical which could affect the stereochemistry of homolytic addition, see: Kaplan, L. "Bridged Free Radicals"; Marcel Dekker: New York, 1972.

(34) For the stabilization of radical ions under these conditions, see: (a) Kaiser, E. T.; Kevan, L., Eds. "Radical Ions"; Interscience: New York, 1968. (b) Hiratsuka, H.; Tanizaki, Y. *J. Phys. Chem.* **1979**, *83*, 2501. (c) Shida, T.; Iwata, S. *J. Am. Chem. Soc.* **1973**, *95*, 3473.

(35) Aromatic cation radicals are known to be photochemically unstable. See ref 34 and 36.

(36) Kholmogorov, V. E.; Gorodyskii, V. A. *Zh. Fiz. Khim.* **1972**, *46*, 63.

complexes of anthracenes, the photophysics of the CT excitation are the same—in both systems charge-transfer excitation leads to the donor–acceptor ion pair [$D^{+}\cdot$, $A^{-}\cdot$]. The difference in the photochemical efficiency arises largely from the nature of the acceptor anion $A^{-}\cdot$. With TCNE, the energetics are such as to allow back electron transfers from $TCNE^{-}\cdot$ to $An^{+}\cdot$ in the ion pair to be the dominant mechanism for relaxation. By contrast, the facile unimolecular fragmentation of $TNM^{-}\cdot$ is sufficiently fast to compete with back-electron transfer; and the photochemistry evolves with high quantum yields from the further spontaneous reactions of the caged fragments [$C(NO_2)_3^{-}$, NO_2, $An^{+}\cdot$], as delineated in Scheme I. In a more general context, the CT mechanism which we have established for the reactions of anthracene–TNM complexes bears directly on a variety of other photoreactions induced by CT excitation or excited-state quenching.[37]

Experimental Section

Materials. Tetranitromethane (Aldrich) was purified by the method of Bielski and Allen.[38] Anthracene, 9-cyanoanthracene, 9-acetylanthracene, and 9-chloroanthracene from Aldrich were each crystallized from ethanol. 9-Phenylanthracene (Aldrich gold label) and 9,10-dimethylanthracene (Aldrich) were used as received. 9-Bromoanthracene and 9-anthraldehyde from Aldrich were each purified by repeated crystallizations from ethanol.[39] 9-Methoxyanthracene,[40] 9-nitroanthracene,[41] methyl 9-anthranoate,[42] 9-anthryl acetate,[40] and 9,10-dimethoxyanthracene[43] were prepared according to the methods described in the literature. The solvents chloroform (Fisher), *n*-pentane (Matheson, Coleman and Bell), and cyclohexane (Matheson, Coleman and Bell) were each dried over molecular sieves (Linde 5A) and distilled under argon prior to use. Methylene chloride (Aldrich gold label) was used as received.

Instrumentation. A Hewlett-Packard HP 8450A diode-array spectrometer was used to obtain the UV–vis spectra. NMR spectra were taken on a Nicolet NT 360 (360 MHz) spectrometer in the FT mode (1-s delay between pulses) with use of dilute solutions in chloroform-*d*, dichloromethane-d_2, or acetonitrile-d_3. Chemical shifts are reported in ppm upfield from Me_4Si vs. internal chloroform (δ 7.26) in the following form: chemical shift (multiplicity, integration, apparent coupling constants in Hz), where s = singlet, d = doublet, t = triplet, m = unresolved multiplet, and b = broadened. A Perkin-Elmer Model 298 spectrophotometer was used to obtain IR spectra of KBr pellets or Nujol mulls. Melting points were taken in capillary tubes with a Mel-Temp (Laboratory Devices) apparatus. The presence of paramagnetic species was probed on a Varian E110 EPR spectrometer. Photochemical irradiations were performed with a focussed 500-W xenon lamp through Corning glass sharp cutoff filters No. 3–69 (500 nm) or No. 2–63 (560 nm) or Edmund interference filters which transmit at 480 ± 10 nm to assure the selective and specific CT excitation of the EDA complexes.

The picosecond laser system for the transient absorption data has been described previously.[17] A single 25-ps (fwhm) pulse (~1 mJ) was selected electrooptically from the pulse train generated from a Nd^{3+}:YAG passively mode-locked oscillator. This 1064-nm pulse was amplified by two Nd^{3+}:YAG amplifiers and converted to 532-nm light with use of a second harmonic generating crystal. A fourth harmonic generating crystal was used with the residual 1064-nm laser pulse to generate the 266-nm pulse.

Determination of Quantum Yields. Quantum yields were measured with a 500-W xenon lamp focussed through aqueous and IR heat filters, followed by a 480-nm interference filter (10-nm band-pass), used as a monochromator. Samples containing 0.050 M of the anthracene and either 0.050 or 0.50 M of TNM in 1.0 mL of deaerated CH_2Cl_2 were irradiated for periods of 0.5 to 5.0 min at room temperature (~22 °C). The CT absorptions of the EDA complexes were monitored periodically by UV spectroscopy. The decrease in intensity of the arene absorptions between 350 and 400 nm also could be monitored after appropriate (250-fold) dilution. Conversions were kept to less than 10%. Potassium ferrioxalate and Reinecke's salt were used as actinometers.[44] The decrease in the CT absorptions of the EDA complexes were about twice the decrease in the absorptions of the arenes. The consumption of TNM was approximately the same as the consumption of the anthracenes listed in Table II.

Formation Constants of EDA Complexes. The formation constants of the EDA complexes from arene–TCNE and arene–TNM were determined with the aid of the Benesi–Hildebrand equation.[45] Since the Benesi–Hildebrand procedure is relatively insensitive to the presence of higher-order complexes,[2] measurements were taken in duplicate under conditions in which the acceptor was present in at least tenfold excess. The temperature in the cuvette was maintained at 23.8 ± 0.2 °C with a Hewlett-Packard 89100A temperature controller. Typical experiments involved concentrations of donors between 0.20 and 0.015 M with 1.5×10^{-3} M TCNE or 2.0×10^{-3} M TNM, concentrations of TCNE between 0.10 and 0.030 M with 2.0×10^{-3} M donor, or concentrations of TNM between 0.40 and 0.080 M with 0.040 M donor in CH_2Cl_2. In one experiment, the concentration of TNM was maintained at 0.020 M and that of anthracene was varied between 0.065 and 0.13 M. The TCNE complexes were monitored at their maximum absorption. The TNM complexes, for which no maxima were apparent, were measured at 500 nm where the uncomplexed starting materials are transparent. Owing to the small values of the absorbances involved ($A < 0.02$) care was taken to ensure that the EDA complexes were the sole absorbing species and that the base line did not change at the monitoring wavelengths selected. Within experimental error, the slopes and intercepts obtained were independent of wavelength. Each plot involved 9–11 points, and linear fits with correlation coefficients of essentially unity were obtained by the method of least squares. However, the slopes of the regression lines were consistently larger when the donor was used in higher concentration than when the acceptor was in access. Although with TCNE the difference in the slope was only 10%, with TNM the slopes differed by about a factor of 2. The greater slopes obtained at higher donor concentrations signify the presence of an additional termolecular component under these conditions.[12]

Procedures for the Matrix Experiments. Irradiations performed in glasses at 77 K produced the blue color of the anthracene radical cations only when the solutions were sufficiently concentrated in An and TNM to produce the EDA complex in amounts which exhibited significant absorbance at the excitation wavelength. Ether–isopentane–alcohol (EPA) was superior to methylcyclohexane at the high concentrations of donor and acceptor required to fulfill this condition. Intense absorptions arising from $An^{+}\cdot$ and II appeared in the spectral region 700–800 and 500 nm, respectively, after brief irradiation (~20 s). In the EPA glasses, thawing resulted in the bleaching of these absorptions. A complex mixture of products was obtained with 9-phenyl-, 9-bromo-, and 9-nitroanthracene, but the photoadducts I (R = Ph, Br, NO_2) were nonetheless formed in substantial amounts (20–40%). Prolonged irradiation at 77 K led to the bleaching of all absorptions which were otherwise stable for indefinite periods if maintained at 77 K. If the solutions were warmed after bleaching, photoadducts I were not observed. Instead, products derived from the oxidation of arene and reaction with EPA solvent were found.[35] Generally, the yields of the photoadducts I were higher when air was excluded from the system. However, we found the reactions to be rather insensitive to the presence of dioxygen when irradiations were performed above 0 °C.

Photochemistry of the EDA Complexes. Procedure for Product Isolation. A concentrated solution of the anthracene (saturated or >0.1 M) and 1.2 equiv of TNM in methylene chloride, *n*-pentane, or cyclohexane was maintained at 10–15 °C in a water-filled Pyrex dewar. The solution was irradiated with light from either a xenon or mercury high-pressure lamp which was passed through a Corning No. 3–69 glass sharp cutoff

(37) (a) Gassman, P. G.; Smith, J. L. *J. Org. Chem.* **1983**, *48*, 4439. (b) Roth, H. D.; Schilling, M. L. M. *J. Am. Chem. Soc.* **1983**, *105*, 6805; **1981**, *103*, 7210. Roth, H. D.; Schilling, M. L. M.; Raghavachari, K. *Ibid.* **1984**, *106*, 253. (c) Barber, R. A.; de Mayo, P.; Okada, K.; Wong, S. K.; *Ibid.* **1982**, *104*, 4995. (d) Jones, G., II; Becker, W. G.; Chiang, S. H. *Ibid.* **1983**, *105*, 1269. Jones, G., II.; Becker, W. G. *Ibid.* **1983**, *105*, 1276. (e) Mukai, T.; Sato, K.; Yamashita, Y. *Ibid.* **1981**, *103*, 670. (f) Sakurai, H.; Sakamoto, K.; Kira, M. *Chem. Lett.* **1984**, 1213. (g) Ng, L.; Balaji, V.; Jordan, K. D. *Chem. Phys. Lett.* **1983**, *101*, 171. (h) Fox, M. A.; Younathan, J.; Fryxell, G. E. *J. Org. Chem.* **1983**, *48*, 3109. (i) Lopez, L.; Calo, V. *J. Chem. Soc., Chem. Commun.* **1984**, 1266. (j) Vermeersch, G.; Marko, J.; Febvay-Garot, N.; Caplain, S.; Lablache-Combier, A. *Tetrahedron* **1978**, *34*, 1493. (k) Carroll, F. A.; Whitten, D. G. *J. Phys. Chem.* **1976**, *80*, 2046. (l) Ware, W. R.; Lewis, C. *Ibid.* **1972**, *57*, 3546.

(38) Bielski, B. H. J.; Allen, A. O. *J. Phys. Chem.* **1967**, *71*, 4544.

(39) A small amount (~1%) of an anthracene impurity remained after this treatment.

(40) Meek, J. S.; Monroe, P. A.; Bouboulis, C. J. *J. Org. Chem.* **1963**, *28*, 2572.

(41) Braun, C. E.; Cook, C. D.; Merritt, C., Jr.; Rousseau, J. E. "Organic Synthesis"; Wiley: New York, 1973, Collect. Vol. IV, p 711.

(42) Parish, R. C.; Stock, L. M. *J. Org. Chem.* **1965**, *30*, 927.

(43) Barnett, E. B.; Cook, J. W.; Mathews, M. A. *J. Chem. Soc.* **1923**, *123*, 1994.

(44) Rabek, J. F. "Experimental Methods in Photochemistry and Photophysics"; Wiley-Interscience: New York, 1982; p 944 ff.

(45) Benesi, H. A.; Hildebrand, J. H. *J. Am. Chem. Soc.* **1948**, *70*, 3978; **1949**, *71*, 2703.

filter until the CT absorptions of the EDA complex were bleached (2-15 min). Crystals of the photoproduct I sometimes formed spontaneously upon irradiation. Concentration of the reaction mixture in vacuo allowed the collection of the major products by filtration. Recrystallization from a mixture of either methylene chloride–carbon tetrachloride or methylene chloride–hexane below room temperature afforded the pure products for characterization. Additional material was obtained by rapid removal of the solvent from the original filtrate and fractional crystallization of the residue. Typically, a solution of 128 mg (0.50 mmol) of 9-bromoanthracene and 100 mg of TNM (0.51 mmol of TNM) dissolved in 5 mL of CH_2Cl_2 was irradiated for ~10 min. The solvent was evaporated and the yellow residue was taken up in ~3 mL of CH_2Cl_2 and ~1 mL of CCl_4 was added. Over a period of several hours, colorless crystals formed which were collected by filtration, washed thrice with small portions of cold CCl_4, and air dried to afford 136 mg (60%) of I (R = Br) as colorless plates. The molecular structures of the photoadducts I with R = Br and Ph were determined by X-ray crystallography at the Molecular Structure Center of Indiana University by Dr. J. C. Huffman. The crystallographic and structural details are contained in the Center reports No. 83066 and No. 83077.

The absorption spectra of the transient arene cation radicals and the trinitromethide anion radical were obtained by the spectroelectrochemical technique with use of the gold minigrid electrode described previously.[18]

Acknowledgment. J. M. Masnovi and J. K. Kochi thank the National Science Foundation and the Robert A. Welch Foundation for financial support. We thank J. C. Huffman for the X-ray crystallographic determination of the photoadducts I shown in Figure 2.

Double Cosets and Enumeration of Permutational Isomers of Fixed Symmetry

Jean Brocas

Contribution from the Collectif de Chimie Organique Physique Faculté des Sciences, Université Libre de Bruxelles, B-1050 Bruxelles, Belgium. *Received December 21, 1984*

Abstract: When a molecular skeleton with n sites and symmetry group G carries n_x ligands of type X, n_y of type Y, etc., the resulting isomers are distributed among several symmetries. We show that the numbers v_γ^{GB} of isomers of symmetry γ obey a system of linear and inhomogeneous equations, as shown by eq 12. The linear coefficients $p_{\beta\gamma}^{G}$ and the independent terms $p_{\beta b}^{S}$ appearing in this system are related to the double-coset structure of G and S_n, respectively, and are easy to calculate by standard group theoretical methods. Unfortunately, the rank of $p_{\beta\gamma}^{G}$ is smaller than the number of v_γ^{GB} unknowns. Hence, the system can only be solved if some of the unknowns are calculated independently. However, in practice, some of the v_γ^{GB} numbers are easy to obtain either because they are vanishing for any ligand partition (phantom subgroups of G) or because they are readily found by inspection, as it is the case when isomers of high symmetry γ have to be enumerated. Therefore, the relations established in this paper do yield an efficient method to enumerate permutational isomers of fixed symmetry. It is remarkable that the calculations required only involve enumeration of double cosets. The present method is applied to the dodecahedrane skeleton. The number of isomers of fixed symmetry and corresponding to the formula $C_{20}H_{20-n}X_n$ have been obtained (n = 0, 1, 2, ..., 10).

I. Introduction

For 15 years, double-coset algebra has been used to enumerate permutational isomers, rearrangements, and reactions. In *static* stereochemistry, the pioneer work is due to Ruch et al.[1] who showed that a permutational isomer (in fact an achiral isomer or a pair of enantiomers) is in one-to-one correspondance with a double-coset Gx_iB in S_n. Here G, B, and S_n are sets of permutations representing, respectively, the group of symmetry operations of the molecular skeleton, the group of permutations of identical ligands, and the symmetric group of degree n (n is the number of sites of the skeleton). The permutation x_i is the representative of Gx_iB and belongs to S_n. In the above paper, the equivalence between the double-coset formalism and Polya's enumeration procedure[2] was also established. For details, notations, and further references, see for instance ref 3.

Group theoretical methods have also been developed to solve the problem of the enumeration of all the distinct stereoisomers of defined constitution. This has been possible by the use of the so-called *configuration* symmetry group.[4]

The importance of double cosets in *dynamic* stereochemistry has been stressed by Hässelbarth and Ruch[5] and by Klemperer.[6-12] These authors showed that the enumeration of permutational and polytopal rearrangements or reactions is again related to double-coset counting. The concept of generalized modes of rearrangements introduced by Nourse[13] is also based on double-coset algebra. This very compact and elegant formalism gives the *total* number (i.e., from every isomer to every isomer) of polytopal rearrangements for a given molecular skeleton and a given ligand partition (for details see for instance ref 3).

The relevance of these mathematical developments to concrete physical and chemical situations has been widely exemplified in the recent literature. In particular, there has been a very strong interaction between the dynamic nuclear magnetic resonance (line-shape analysis) and the permutation description of magnetic site exchange.[3,12,14] The concepts of residual stereoisomerism and stereotopism[15-17] are also related to these algebraic methods. In

(1) Ruch, E.; Hässelbarth, W.; Richter, B. *Theoret. Chim. Acta* **1970**, *19*, 288.
(2) Polyā, G. *Acta Math.* **1937**, *68*, 145, 213.
(3) Brocas, J.; Gielen, M.; Willem, R. "The Permutational Approach to Dynamic Stereochemistry"; McGraw-Hill: New York, 1984.
(4) Nourse, J. G. *J. Am. Chem. Soc.* **1979**, *101*, 1210, 1216.
(5) Hässelbarth, W.; Ruch, E. *Theoret. Chim. Acta* **1973**, *29*, 259.
(6) Klemperer, W. G. *J. Chem. Phys.* **1972**, *56*, 5478.
(7) Klemperer, W. G. *Inorg. Chem.* **1972**, *11*, 2668.
(8) Klemperer, W. G. *J. Am. Chem. Soc.* **1972**, *94*, 6940.
(9) Klemperer, W. G. *J. Am. Chem. Soc.* **1972**, *94*, 8360.
(10) Klemperer, W. G. *J. Am. Chem. Soc.* **1973**, *95*, 380.
(11) Klemperer, W. G. *J. Am. Chem. Soc.* **1973**, *95*, 2105.
(12) Klemperer, W. G. In "Dynamic Nuclear Magnetic Resonance Spectroscopy"; Jackman, L. M., Cotton, F. A., Eds.; Academic Press: New York, 1975.
(13) Nourse, J. G. *J. Am. Chem. Soc.* **1977**, *99*, 2063.
(14) Balasubramanian, K. *J. Phys. Chem.* **1982**, *86*, 4668.
(15) Finocchiaro, P.; Gust, D.; Mislow, K. *J. Am. Chem. Soc.* **1974**, *96*, 3198.
(16) Finocchiaro, P.; Gust, D.; Mislow, K. *J. Am. Chem. Soc.* **1974**, *96*, 3205.

0002-7863/86/1508-1135$01.50/0